Chromatin-associated proteins HMGB1/2 and PDIA3 trigger cellular response to chemotherapy-induced DNA damage

Natalia F. Krynetskaia, Manali S. Phadke, Sachin H. Jadhav, and Evgeny Y. Krynetskiy

Temple University School of Pharmacy, Philadelphia, Pennsylvania

Abstract

The identification of new molecular components of the DNA damage signaling cascade opens novel avenues to enhance the efficacy of chemotherapeutic drugs. High-mobility group protein 1 (HMGB1) is a DNA damage sensor responsive to the incorporation of nonnatural nucleosides into DNA; several nuclear and cytosolic proteins are functionally integrated with HMGB1 in the context of DNA damage response. The functional role of HMGB1 and HMGB1-associated proteins (high-mobility group protein B2, HMGB2; glyceraldehyde-3-phosphate dehydrogenase, GAPDH; protein disulfide isomerase family A member 3, PDIA3; and heat shock 70 kDa protein 8, HSPA8) in DNA damage response was assessed in human carcinoma cells A549 and UO31 by transient knockdown with short interfering RNAs. Using the cell proliferation assay, we found that knockdown of HMGB1-associated proteins resulted in 8-fold to 50-fold decreased chemosensitivity of A549 cells to cytarabine. Western blot analysis and immunofluorescent microscopy were used to evaluate genotoxic stress markers in knocked-down cancer cells after 24 to 72 hours of incubation with 1 μmol/L of cytarabine. Our results dissect the roles of HMGB1-associated proteins in DNA damage response: HMGB1 and HMGB2 facilitate p53 phosphorylation after exposure to genotoxic stress, and PDIA3 has been found essential for H2AX phosphorylation (no γ-H2AX accumulated after 24–72 hours of incubation with 1 μmol/L of cytarabine in PDIA3 knockdown cells). We conclude that phosphorylation of p53 and phosphorylation of H2AX occur in two distinct branches of the DNA damage response. These findings identify new molecular components of the DNA damage signaling cascade and provide novel promising targets for chemotherapeutic intervention. [Mol Cancer Ther 2009;8(4):864–72]

Introduction

Traditional chemotherapeutic agents targeted against DNA remain the core of anticancer therapy, and several million people worldwide receive conventional chemotherapeutics yearly (1). The efficacy of these drugs is limited partly because of cellular mechanisms that diminish DNA damage by executing cell cycle arrest and DNA repair (2).

High-mobility group protein B1 (HMGB1) is an architectural transcription factor, and a component of the early DNA damage sensor responsive to the incorporation of nonnatural nucleosides into DNA that occurs without compromising DNA integrity (3–5). HMGB1 binds flexible DNA (prone to acquire bent or kinked conformation), rather than DNA with single-stranded or double-stranded breaks, and recruits other proteins to the DNA-HMGB1 complex (3). In murine embryonic fibroblasts, knockout of HMGB1 decreased sensitivity to antimetabolites 5-fold to 10-fold, and inhibited the activation of p53-mediated response to genotoxic stress (5).

Initial identification of HMGB1 as a DNA damage–sensing protein revealed a group of proteins (high-mobility group protein B2, HMGB2; glyceraldehyde-3-phosphate dehydrogenase, GAPDH; protein disulfide isomerase family A, member 3, PDIA3; and heat shock 70 kDa protein 8, HSPA8) which were physically associated with HMGB1 (4). Although HMGB2 is a structural analogue of HMGB1 with amino acid sequence >85% identical to that of HMGB1, knockout of this protein in mice confers a phenotype quite distinct from that of Hmgb1-knockout mice (6). The role of HMGB2 in DNA damage stress response remained uncharacterized. Cytosolic proteins GAPDH and PDIA3 have been recently recognized to have intranuclear functions, and now are the focus of intensive studies (7, 8). Intranuclear localization and molecular partners of PDIA3 (also known as ERp60, ERp57, or GRP58) suggests its participation in DNA repair processes (8, 9). Finally, HSPA8 (also known as HSC70) is a molecular chaperone involved in intranuclear translocation of cytosolic proteins. In response to different types of stress, including heat shock and oxidative stress, HSPA8 accumulates in the nucleolus, although its functions still remain to be elucidated (10, 11).

Recently, novel inhibitors of the cellular mechanisms responsive to DNA damage have been developed and entered into clinical trials (12, 13). Within this approach, the cellular components involved in the activation of chemotherapy-induced DNA damage response provide important targets because inhibition of checkpoints that regulate cell division and limit DNA damage can potentiate the efficiency of

Received 7/22/08; revised 1/6/09; accepted 2/2/09; published OnlineFirst 4/9/09.

Grant support: National Cancer Institute grant R01-CA104729 (E. Krynetskiy).

The costs of publication of this article were defrayed in part by the payment of page charges. This article must therefore be hereby marked *advertisement* in accordance with 18 U.S.C. Section 1734 solely to indicate this fact.

Requests for reprints: Evgeny Krynetskiy, Temple University School of Pharmacy, 3307 North Broad Street, Philadelphia, PA 19140. Phone: 215-707-4257; Fax: 215-707-3678. E-mail: ekrynets@temple.edu

doi:10.1158/1535-7163.MCT-08-0695

chemotherapy. This is especially true with respect to antimetabolite drugs known to incorporate into DNA without gross changes of the DNA structure (14, 15).

The primary focus of our study is to test the hypothesis that HMGB1 and associated proteins are involved in cellular response to antimetabolite drugs. Multiple publications have shown that antimetabolite treatment induced p53-mediated apoptotic death of cells via genotoxic stress, although the beginning of this pathway remains obscure. In the present study, we set out to characterize the functional role of HMGB1-associated proteins in the early steps of DNA damage response to chemotherapeutic agents, at the cellular level. To this end, we used a model system based on human carcinoma cells in which individual proteins including HMGB1, HMGB2, GAPDH, PDIA3, and HSPA8 were knocked down by short interfering RNA (siRNA) treatment. Our studies showed that the homologous proteins HMGB1 and HMGB2 participate in DNA damage response by modulating p53 phosphorylation. We also found that, after chemotherapy-induced stress, the cytosolic proteins PDIA3 and HSPA8 accumulate in the nucleus; importantly, our data indicate that intranuclear PDIA3 modulates the phosphorylation of H2AX histone.

Therefore, for the first time, we showed the functional role of HMGB1-associated proteins HMGB1, HMGB2, and PDIA3 in chemotherapy-induced DNA damage stress response in human cancer cells. Together, these findings identify molecular components of the DNA damage signaling cascade and provide novel promising targets for chemotherapeutic intervention.

Materials and Methods

Cell Cultures, Drug Treatment, and Plasmids

Lung carcinoma cells A549 were obtained from the American Type Culture Collection, and renal carcinoma UO31 cells were obtained from the Tumor Cell Line Repository, NCI-Frederick. Cells were treated with drugs dissolved in DMSO (fluorouracil), 0.1 N NaOH (mercaptopurine), or water (cytarabine) as 500× to 1,000× stock solutions; drug concentrations were determined spectrophotometrically (fluorouracil, ε_{265} = 7,010; mercaptopurine, ε_{320} = 19,600; cytarabine, ε_{272} = 9,259; ref. 16). [5-^{3}H]Cytosine-β-D-arabinofuranoside (14.9 Ci/mmol; Moravek Biochemicals) was used in DNA incorporation experiments. The IC_{50} values were calculated by fitting a sigmoid E_{max} model to the cell viability versus drug concentration data, determined in triplicate from three independent experiments.

Cell Growth and Viability

Cell viability and cell count were determined by flow cytometry using ViaCount reagent with Guava Personal Cell Analyzer (Guava Technologies). Clonogenic assay was done after cell treatment for 3 d, cell growth for 10 d, and staining with methylene blue (17). For the 3-(4,5-dimethylthiazol-2-yl)-2,5-diphenyltetrazolium (MTT) assay (CellTiter 96 cell proliferation kit; Promega), A549 and UO31 cells (250 cells/well) were plated into 96-well plates, and cultured for 3 to 5 d in varying concentrations of the following drugs: 0 to 100 μmol/L of mercaptopurine, 0 to 50 μmol/L of cytarabine, and 0 to 100 μmol/L of fluorouracil.

RNA Interference with Short Duplex RNA

RNA interference experiments were done using the predesigned Stealth RNA (Invitrogen; HMGB1—HSS142453, HSS142454, HSS142455; HMGB2—HSS104854, HSS104855, HSS104856; GAPDH Validated Stealth RNAi DuoPak duplexes 1 and 2; PDIA3—HSS142315, HSS142316, HSS142317; and HSPA8—HSS105082, HSS105083, HSS105084). Effective siRNA were selected using a lac-Z reporter system (BLOCK-iT RNAi Target Screening System; Invitrogen). Scrambled Negative Stealth RNAi control (Invitrogen) was used as a negative control in all siRNA experiments.

Analysis of mRNA Expression by Real-time PCR

Total cellular RNA was extracted with TriReagent (Life Technologies/Invitrogen) from A549 and UO31 cells (~5 × 10^6 cells per experiment, three replicates), reverse transcribed using the TaqMan Reverse Transcription kit (Applied Biosystems) according to the instructions of the manufacturer. The level of mRNA was evaluated using Relative Quantification protocol with human β-actin as a normalization standard on ABI 7300 Real-time PCR instrument (Applied Biosystems) according to the instructions of the manufacturer. Data were collected from three independent experiments for each sample.

Western analysis was done as described earlier (4). The subcellular fractionation into cytosolic and nuclear fractions was done using NE-PER Extraction reagent (Pierce Biotechnology) according to the instructions of the manufacturer. The protein concentration was determined in cellular extracts using PlusOne 2D Quant kit (Amersham Biosciences). Electrophoretic separation was done using 16% PAGE gels for analysis of γ-H2AX, HMGB1, and HMGB2; 12% PAGE gels for analysis of phosphorylated p53; and gradient 4% to 12% PAGE gels for analysis of PARP, PDIA3, and HSPA8 (PageGel). Membranes were developed with rabbit polyclonal antibodies specific to HMGB1 at 1:1,000 dilution and HMGB2 at 1:500 dilution (Abcam); rat anti-HSPA8 monoclonal antibody at 1:5,000 dilution (Stressgen); rabbit anti-GAPDH polyclonal antibody at 1:10,000 dilution (Santa Cruz Biotechnology); rabbit anti-PDIA3 polyclonal antibody (Rockland) were generated as described earlier and used at 1:5,000 dilution (4); rabbit anti–Ser^{15} phosphorylated p53 polyclonal antibody at 1:1,000 dilution and rabbit anti–γ-H2AX (H2AX phosphorylated at Ser^{139}) polyclonal antibody at 1:500 dilution (Calbiochem); rabbit anti-PARP polyclonal antibody at 1:1,000 dilution (Cell Signaling Technology); rabbit anti–85 kDa PARP fragment polyclonal antibody at 1:500 dilution (Abcam); and mouse anti–β-actin monoclonal antibody (loading control) at 1:10,000 dilution (Sigma). Bands were visualized with secondary antibody—IRDye680 donkey anti-mouse antibody and IRDye680 goat anti-rabbit antibody; or IRDye 800CW donkey anti-rabbit antibody (LI-COR Biosciences) and IRDye 800CW goat anti-rat antibody (Rockland) at 1:10,000 dilution and quantified by Odyssey Infrared Imaging system (LI-COR Biosciences) using two-color fluorescence detection at 700 and 800 nm.

Immunofluorescent Microscopy

Cells were grown on BD BioCoat poly-L-lysine precoated glass coverslips (Thermo Fisher Scientific) in 12-well plates at a density of 50,000 cells/well, treated with 10 μmol/L of cytarabine for 48 h and fixed in 4% formaldehyde in PBS for 15 min. Cells were then washed in ice-cold methanol, blocked in 5% normal rabbit serum, and labeled with anti–γ-H2AX antibody (phosphorylated histone H2A.X rabbit monoclonal antibody conjugated with Alexa Fluor 488; Cell Signaling Technology). The slides were incubated with anti–phosphorylated histone H2A.X antibody (1:10 dilution) overnight at 4°C. Nuclei were counterstained with 4′,6′-diamidino-2-phenylindole and mounted with Vectashield hard set mounting medium (Vector Laboratories). Fluorescence images were recorded with a Nikon Eclipse 50 fluorescent microscope and analyzed by ImageJ 1.37v software (NIH). All experiments were repeated at least four times. At least 100 cells were analyzed in each experiment.

Caspase Activation

A549 and UO31 cells were grown in 96-well plates in Ham's F12K or RPMI 1640 and treated with 10 μmol/L of fluorouracil, 10 μmol/L of mercaptopurine, or 0.5 μmol/L of cytarabine for 24 to 48 h. Actinomycin D (0.5 μg/mL) was used as a positive control. Caspase activity was assessed using fluorogenic substrates for caspase 3 and caspase 7 using Apo-ONE Homogenous Caspase 3/7 Assay, according to the instructions of the manufacturer (Promega). Caspase activity was normalized per milligram of total protein, and compared with activity in nontreated cells. Each experiment was done in triplicate and repeated at least thrice.

Statistical Analysis

The statistical analyses were carried out using Student's *t* test with Statistica software program (StatSoft), and nonlinear regression analysis with GraphPad Prism 4.0 software (GraphPad software). $P < 0.05$ was considered statistically significant. Data are presented as the mean ± SE.

Results

Antimetabolite Treatment Decreases Cell Proliferation and Clonogenic Survival in Carcinoma Cells A549 and UO31

Two human carcinoma cell lines (lung carcinoma A549 and renal carcinoma UO31) proficient in p53-dependent DNA damage response pathway were selected as a model system for the analysis of cellular response to antimetabolite drugs (18). Both cell lines were easily transfected with siRNA, and revealed effective knockdown of targeted proteins within 24 to 48 hours (see below). To assess the chemosensitivity of the model cell lines, we used clonogenic and MTT assays. Although the clonogenic potential of A549 cells was readily measured after drug treatment, UO31 cells did not form colonies and were therefore excluded from clonogenic assays. Clonogenic survival of A549 was decreased following treatment with 0 to 50 μmol/L of cytarabine, and 0 to 100 μmol/L of fluorouracil but not after 0 to 100 μmol/L of mercaptopurine treatment; cytarabine was the most potent cytotoxic agent for A549 cells (Fig. 1A; Table S1).[1]

Furthermore, sensitivity of A549 and UO31 to antimetabolites was evaluated by the MTT assay indicative both of cytotoxic and cytostatic effects (19). After 24 to 72 hours of treatment with 0 to 100 μmol/L of fluorouracil, A549 and UO31 cells showed decreased MTT reducing activity; both cells were most sensitive to cytarabine treatment (Fig. 1C; Table S1).[1] Similar to the results from clonogenic assays, A549 was found to be resistant to mercaptopurine treatment in the range 1 to 100 μmol/L (data not shown); UO31 was sensitive to this drug (IC_{50} = 2.3 ± 0.55 μmol/L) indicating that metabolic activation of mercaptopurine in UO31 cells is functional.

Antimetabolite Treatment Induces Apoptosis in Carcinoma Cells A549 and UO31

Activation of apoptosis in the A549 and UO31 cell lines was tested after treatment with three antimetabolite drugs (mercaptopurine, fluorouracil, and cytarabine) at concentrations 5 to 10 times higher than IC_{50}. After treatment with 10 to 50 μmol/L of fluorouracil, we did not observe caspase activation or PARP proteolysis in either A549 or UO31 cells (Fig. 1B and D), although fluorouracil treatment had a growth-inhibiting effect both on A549 and UO31 (results not shown). Mercaptopurine (10 μmol/L) was a weak inducer of apoptosis in UO31 (Fig. 1D). Treatment with cytarabine at concentrations 5 to 10 times above the IC_{50} values induced apoptotic death in both cell lines after 48 hours of incubation, as revealed by the activation of apoptotic markers (proteolysis of caspase 3 substrate PARP; Fig. 1B, and 2-fold to 4-fold induction of caspases 3/7 activity; Fig. 1D). Because incorporation in DNA is a major mechanism of cytarabine cytotoxicity, we verified the ability of both cell lines to use cytarabine as a DNA precursor. Incorporation of cytarabine into DNA was evaluated using [5-^{3}H]cytarabine; these experiments confirmed that cytarabine was incorporated into the DNA of both cell lines at comparable levels (0.1–0.5%) and was already detectable after 24 hours of incubation (Fig. S1).[1] Therefore, in further experiments, we used cytarabine treatment to assess cytotoxic effects in A549 and UO31 cells with knockdown proteins.

Knockdown of HMGB1-Associated Proteins Using RNA Interference

Western blot analysis showed that both cell lines were proficient in expressing HMGB1, HMGB2, GAPDH, PDIA3, and HSPA8 proteins (Fig. 2A). To assess the role of HMGB1-associated proteins in genotoxic stress response, we established a model system based on siRNA technology. This transient knockdown system made it possible to rapidly test the functional role of five HMGB1-associated proteins in response to genotoxic stress caused by nucleoside analogues. The selection of an efficient siRNA targeted against mRNAs coding for HMGB1-associated proteins was done in an A549 cell line using a siRNA screening system; the efficiency of siRNA-mediated mRNA knockdown estimated by

[1] Supplementary data for this article are available at Molecular Cancer Therapeutics Online (http://mct.aacrjournals.org/).

real-time PCR was typically >90%. The changes in protein level were monitored by Western blot analysis. siRNA that reduced the protein level by >70% were selected for further analysis. The following siRNA were chosen for knockdown: HMGB1 (HSS142453), HMGB2 (HSS104854), GAPDH (validated Stealth RNAi DuoPak duplex 1), PDIA3 (HSS142316), and HSPA8 (HSS105082). The knockdown effect was evident during the entire experiment (24–72 hours; see Fig. S2).[1] Interestingly, siRNA knockdown was consistently more effective in A549 cells (10–25% of residual protein) compared with UO31 cells (25–40% of residual protein), as evidenced by the lower levels of residual proteins (Fig. 2A and B). Knockdown of HMGB1/2, PDIA, and HSPA8 proteins in A549 and UO31 cells did not significantly change the rate of cell growth compared with negative controls ($P > 0.05$), whereas cell growth arrest was observed in cells with knocked down GAPDH ($P < 0.004$, Table S2).[1]

Knockdown of HMGB1-Associated Proteins Renders Cancer Cell Lines A549 and UO31 More Resistant to Antimetabolites

According to our hypothesis, HMGB1 and associated proteins act at the beginning of the genotoxic stress pathway. We used an MTT assay to test the chemosensitivity of cancer cell lines following knockdown of nuclear proteins associated with HMGB1, to assess short-term effects generated by the DNA damage sensor (Fig. 2C; Table 1). In these experiments, a five-orders of magnitude range of concentrations of cytarabine was used to evaluate its inhibitory effect on cell growth and viability. Importantly, knockdown of HMGB1 and HMGB2 resulted in an 8-fold to 13-fold increase of IC_{50} in A549 cells treated with cytarabine, and a 3-fold to 8-fold increase in UO31. Similar to the effects of HMGB1/2, knockdown of PDIA3 and HSPA8 in A549 resulted in an 8-fold to 10-fold increase of IC_{50} (Table 1). In contrast, PDIA3 and HSPA8 knockdown in UO31 did not alter cell viability (Table 1). Although the levels of these proteins were reduced to 10% to 20% in A549 cells, in UO31, the residual levels were ~30% to 40% (Fig. 2B), providing an explanation for the smaller difference in cytotoxic effects. The strongest effect was achieved by knockdown of GAPDH (>50-fold increase of IC_{50}; see Fig. S3).[1] Because GAPDH knockdown caused cell growth arrest (Table S2),[1] we excluded siGAPDH treatment from further cytotoxicity experiments. Therefore, in experiments on molecular markers of cytotoxicity, we used A549 and UO31 cells with knockdown proteins HMGB1, HMGB2, PDIA3, and HSPA8 after treatment with cytarabine.

Knockdown of HMGB1-Associated Proteins Reduces Markers of DNA Damage and Apoptosis

The levels of phosphorylated S15-p53 (the marker of p53 activation), γ-H2AX (the marker of double-strand break formation), and accumulation of 85 kDa PARP fragment (the

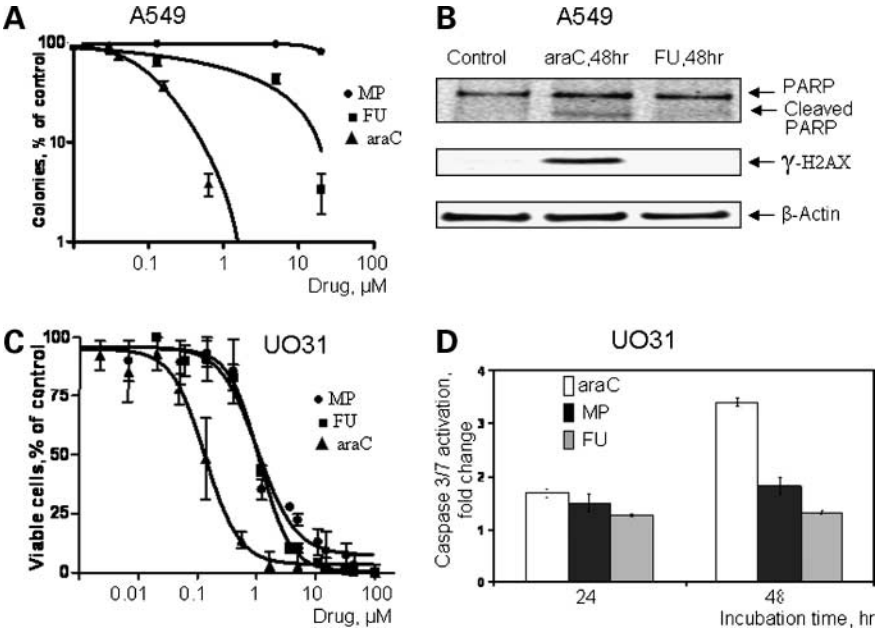

Figure 1. Chemosensitivity of A549 and UO31 cells to a panel of antimetabolite drugs. **A,** the chemosensitivity of A549 cells was evaluated by clonogenic assay. A549 cells were treated with six consecutive dilutions of fluorouracil (*FU*), cytarabine (*araC*), or mercaptopurine (*MP*) for 3 d, trypsinized, and seeded in 100 mm Petri dishes. *Points,* mean of clonogenic data from three independent experiments, with three dishes per dose; *bars,* SE (where not seen, the bars are smaller than the symbol). **B,** Western blot analysis of protein extracts from A549 cells treated with 1 μmol/L of cytarabine and 10 μmol/L of fluorouracil for 48 h and developed with anti-PARP antibody (*top*) or anti–γ-H2AX antibody (*middle*). *Arrows,* positions of the 85 kDa cleaved PARP fragment, and γ-H2AX, correspondingly. β-Actin was used as a loading control. **C,** the chemosensitivity of UO31 cells was evaluated by MTT assay using nine consecutive dilutions of antimetabolite drugs after 5 d of incubation. *Curves,* results of three independent experiments, with two duplicates in each experiment. **D,** caspase 3/7 activation following treatment of UO31 cells with 1 μmol/L of cytarabine, 10 μmol/L of mercaptopurine, and 10 μmol/L of fluorouracil for 24 to 48 h. Activity was normalized versus caspase activity at the zero time point (no drug added). Data from three independent experiments.

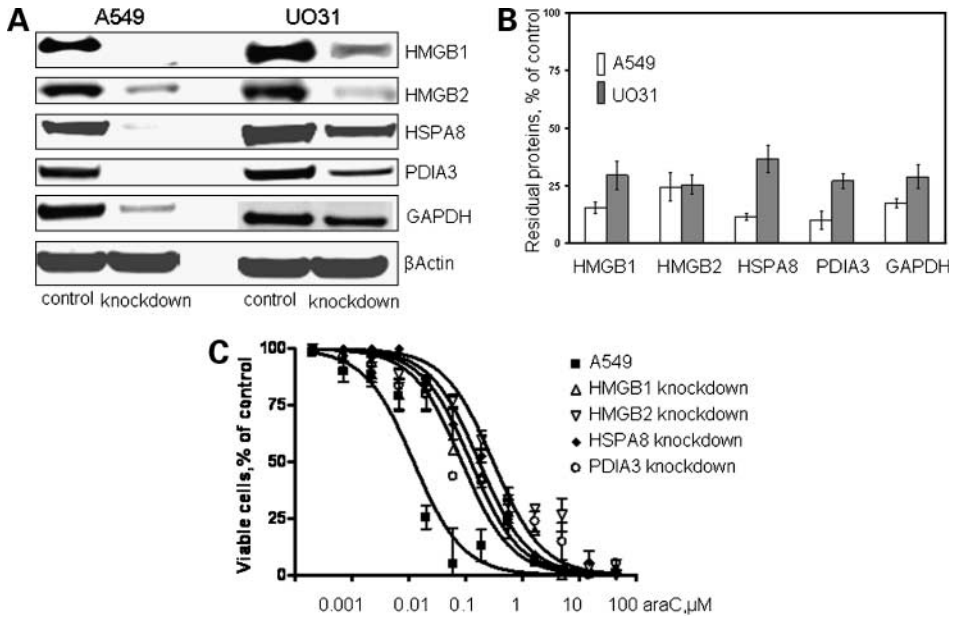

Figure 2. Treatment of A549 and UO31 cells with siRNA against HMGB1, HMGB2, GAPDH, PDIA3, and HSPA8 mRNAs resulted in the knockdown of target proteins, and increased resistance to drug treatment. **A,** Western blot analysis of 40 μg total protein extracts after transfection with siRNA and incubation for 48 h in A549 and UO31 cell lines. For analysis of HMGB2 in A549 cells, 80 μg of total protein was loaded per lane. Electrophoretic separation was done using 16% (HMGB1/2 proteins), 12% (GAPDH), and gradient 4% to 12% PAGE gels (PDIA3 and HSPA8 proteins). For details of Western analysis, see Materials and Methods. **B,** quantification of Western blots done by scanning and image analysis after incubation with chromophore-labeled secondary antibody. β-Actin was used as a loading control. Scrambled siRNA was used as negative control in all experiments. **C,** knockdown of HMGB1-associated proteins increases the resistance of A549 to cytarabine (*araC*) as determined by MTT assay. A549 cells were treated with siRNA: siHMGB1, siHMGB2, siPDIA3, siHSPA8. After 48 h of incubation, cells were trypsinized and seeded in 96-well plates at a density of 250 cells/well. Cells were treated by consecutive dilutions of cytarabine (0–50 μmol/L), and incubated for 3 d before collecting data. For all four siRNA-treated cells, results were statistically significantly different from the control cells transfected with scrambled siRNA ($P < 0.0025$).

marker of caspase 3 activation) were monitored to assess the effects of knockdown of HMGB1-associated proteins. After transfection with siRNA targeted against HMGB1, HMGB2, PDIA3, and HSPA8, both A549 and UO31 cells were treated with 1 μmol/L of cytarabine for 24 to 72 hours, and cell lysates were analyzed by Western blotting (Fig. 3). Accumulation of the Ser^{15}-phosphorylated form of p53 was already notable after 24 hours of incubation in control cells (transfected with scrambled siRNA), but it was delayed till 48 to 72 hours in cells with knocked down HMGB1 and HMGB2, corroborating the functional role of these proteins in cellular response. Knockdown of HMGB1/2, which delayed the accumulation of the S15-p53 level, also slightly affected the formation of γ-H2AX (Fig. 3). Importantly, accumulation of Ser^{15}-phosphorylated p53 (Fig. 3A and C) paralleled the accumulation of the 85 kDa PARP fragment, indicative of caspase 3 activation (Fig. 4A and B). The most pronounced drop in the accumulation of the 85 kDa PARP fragment was observed in cells with reduced HSPA8 protein; this finding is still awaiting explanation (Fig. 4A and B).

Western blot analysis of cytosolic and nuclear extracts isolated from untreated A549 cells showed that PDIA3 and HSPA8 reside in the cytosol. These proteins relocate into the nuclei after cytarabine treatment (Fig. 5; Fig. S4).[1] Figure 5B shows accumulation of PDIA3 in the nucleus of cells following incubation with 1 μmol/L of cytarabine for 24 to 72 hours. In A549/siPDIA3 knockdown cells, the total level of PDIA3 was reduced by 90% (Fig. 2B), and its accumulation in the nucleus of siPDIA3-treated A549 cells in response to drug treatment was notable after 72 hours of incubation (Fig. 5B).

Table 1. Cytotoxic effects of cytarabine after knockdown of HMGB1-associated proteins HMGB1, HMGB2, GAPDH, PDIA3, and HSPA8 in A549 and UO31 cell lines measured by MTT assay (IC_{50} ± SE)

siRNA	Cell line	IC_{50} ± SE, μmol/L
Scrambled	A549	0.03 ± 0.015
SiHMGB1	A549	0.25 ± 0.051
SiHMGB2	A549	0.39 ± 0.062
GAPDH	A549	1.68 ± 0.182
PDIA3	A549	0.24 ± 0.019
HSPA8	A549	0.3 ± 0.028
Scrambled	UO31	0.07 ± 0.095
SiHMGB1	UO31	0.24 ± 0.027
SiHMGB2	UO31	0.22 ± 0.049
GAPDH	UO31	>100
PDIA3	UO31	0.08 ± 0.045
HSPA8	UO31	0.09 ± 0.015

NOTE: Data points were collected after a 72-h incubation with 0 to 50 μmol/L of cytarabine.

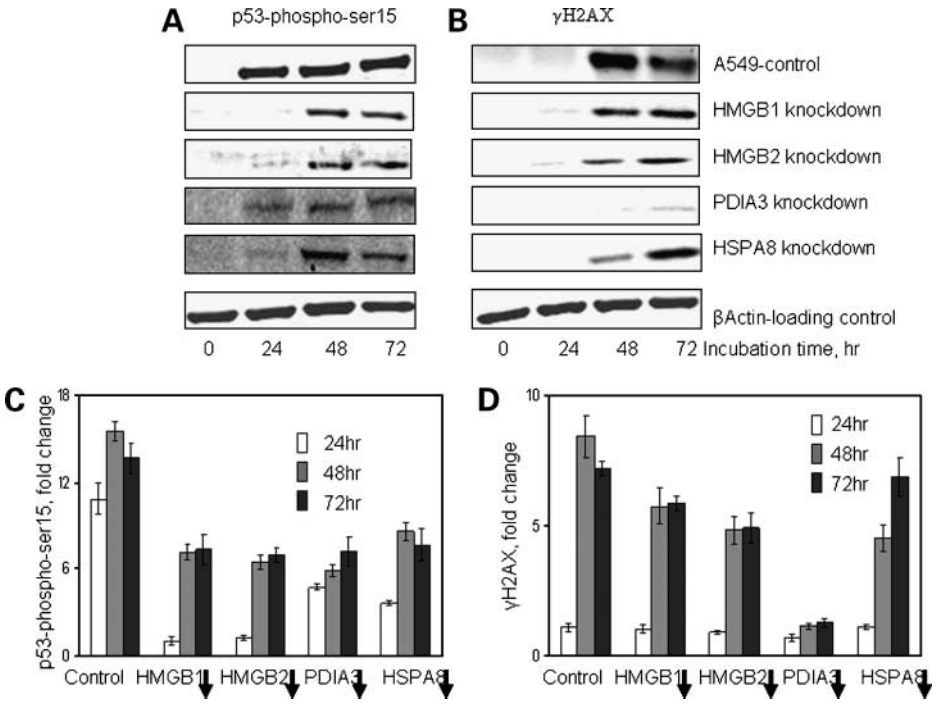

Figure 3. Accumulation of p53 phosphorylated at Ser^{15} (**A** and **C**), and H2AX phosphorylated at Ser^{139} (**B** and **D**). After transfection with corresponding siRNA, cells were incubated for 48 h, trypsinized, and seeded at a density of 5,300 cells/cm^2. The next day, 1 μmol/L of cytarabine was added; nuclear extracts were prepared at 0, 24, 48, and 72 h in the presence of protease and protein phosphatase inhibitors, and analyzed by Western blot analysis under conditions indicated in Materials and Methods. Experiments were repeated three to four times, and quantification was done by scanning and image analysis after incubation with chromophore-labeled secondary antibody. β-Actin was used as a loading control. Scrambled siRNA was used as negative control in all experiments.

Interestingly, knockdown of PDIA3 protein in A549 cells inhibited the accumulation of γ-H2AX following cytarabine treatment (Fig. 3B and D). Under the same conditions, phosphorylation of Ser^{15} in p53 was already observed after 24 hours of incubation, indicating that phosphorylation of p53 and H2AX are independent events (Fig. 3). To corroborate these data, we evaluated the formation of γ-H2AX foci in A549/siPDIA3 cells treated with cytarabine by immunofluorescent microscopy (Fig. 5A). Cells treated with hydroxyurea were used as positive controls (Fig. S5;[1] ref. 20). A significantly lower number of cells treated with cytarabine were stained with anti–γ-H2AX antibody when PDIA3 protein was knocked down (Fig. 5A), consistent with the results of Western blot analysis (Fig. 3B and D). In parallel to inhibition of H2AX phosphorylation, accumulation of 85 kDa PARP fragment in the cells with knocked down PDIA3 protein occurred with a delay compared with control cells (Fig. 4A and B). The same effects were observed in UO31 cells after the knockdown of HMGB1-associated proteins (data not shown).

Discussion

The role of HMGB1 in recognizing aberrant or damaged DNA has been shown in multiple *in vitro* experiments. A recent study directly showed the accumulation of HMGB1 at sites of oxidative DNA damage in live cells thus defining HMGB1 as a component of an early DNA damage response (21). Reduced histone acetylation after DNA damage in HmgB1-deficient cells indicates a role for HMGB1 in DNA damage–induced chromatin remodeling (22). In the present study, we established a model system based on human carcinoma cells A549 and UO31, in which two groups of

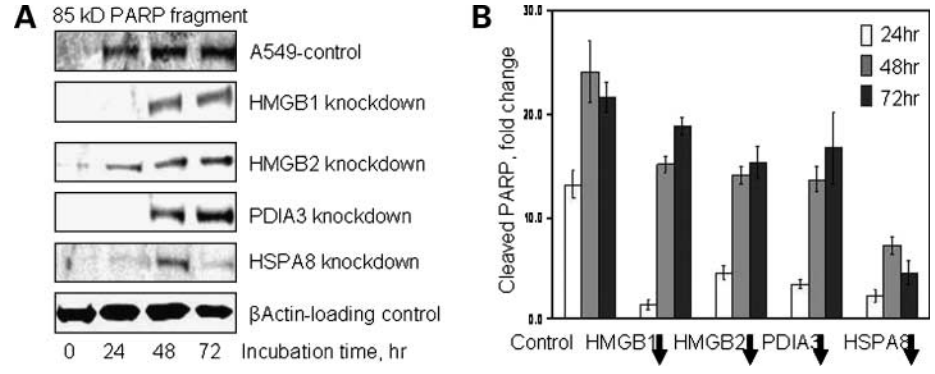

Figure 4. **A** and **B**, activation of caspase-mediated cleavage of PARP in A549 cells after treatment with cytarabine. After transfection with corresponding siRNA, cells were incubated for 48 h, trypsinized, and seeded at a density of 5,300 cells/cm^2. The next day, 1 μmol/L of cytarabine was added; nuclear extracts were prepared at 0, 24, 48, and 72 h in the presence of protease and protein phosphatase inhibitors, and analyzed by Western blot analysis under conditions indicated in Materials and Methods. Quantification was done by scanning and image analysis after incubation with chromophore-labeled secondary antibody.

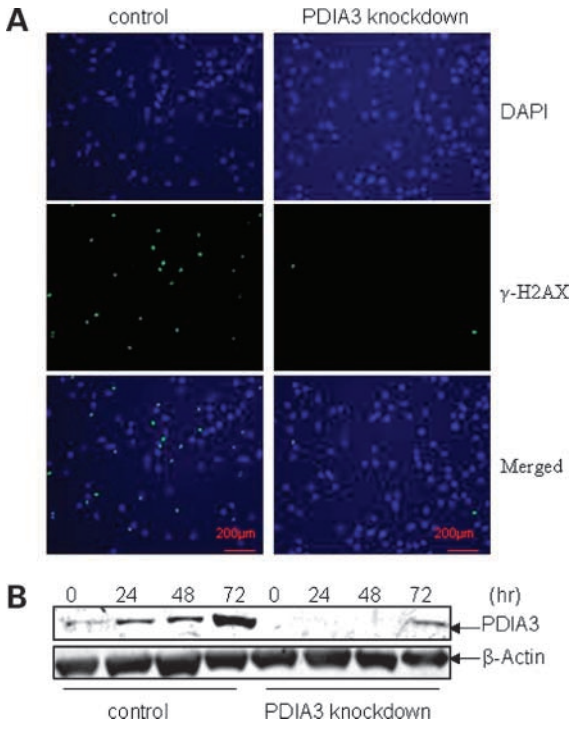

Figure 5. Accumulation of γ-H2AX in A549/siPDIA3 cells after genotoxic stress. **A,** formation of γ-H2AX foci following genotoxic stress. A549 control cells (*left*) or A549/siPDIA3 cells (*right*) were treated with 1 μmol/L of cytarabine for 48 h, fixed with formaldehyde and immunostained with anti–γ-H2AX antibody conjugated with Alexa Fluor 488. After the final wash, cells were counterstained with 4′,6′-diamidino-2-phenylindole and mounted on the slide as described in Materials and Methods. Hydroxyurea was used as a positive control for γ-H2AX foci formation (Fig. S5).[1] **B,** intranuclear accumulation of PDIA3 in A549 control cells and A549/siPDIA3 cells. Nuclei were isolated from 1×10^6 A549 cells treated with scrambled siRNA (*left lanes*) or siPDIA3 (*right lanes*), challenged with 1 μmol/L of cytarabine for 48 h, and analyzed by Western blot analysis using a gradient 4% to 12% PAGE gel. β-Actin was used as a loading control.

proteins—nuclear proteins (HMGB1/2) and proteins transiently present in the nucleus after the drug stress (GAPDH, PDIA3, and HSPA8) were knocked down with siRNA. Because cytarabine was the strongest inducer of apoptosis in both cell lines, we used it to challenge cells following siRNA treatment. The cytotoxic effect of cytarabine is due to incorporation into DNA and is mediated by p53 (12, 23). The cytarabine concentration for cell treatment (1 μmol/L cytarabine) was selected to maximize the effect of the drug at relatively short exposure periods (24–72 hours). This concentration lies within the range of cytarabine plasma concentrations achieved in some protocols for the treatment of hematopoietic malignancies (24).

siRNA treatment effectively decreased the level of proteins in both cell lines, although the residual levels of four proteins (HMGB1, GAPDH, PDIA3, and HSPA8) were consistently higher in UO31 cells compared with A549 cells (Fig. 2). The rate of proliferation of knockdown cells did not change significantly, with the exception of cells treated with siGAPDH, in which this treatment arrested cell growth. This was not unexpected, as GAPDH is involved in cell cycle regulation via interaction with cyclin B (25), and/or S phase–inducible H2B transcription activator OCA-S (26). Depletion of GAPDH in A549 and UO31 cell lines dramatically altered cell chemosensitivity (Table 1; Fig. S3).[1] Because antimetabolite drugs exert their cytotoxic effects during the S phase of the cell cycle, the unusually strong effect of GAPDH knockdown on cell viability is probably the consequence of cell cycle arrest, a hypothesis under investigation in our lab.

Abrogation of HMGB1 and HMGB2 increased chemoresistance both in A549 and UO31 cell lines (Table 1; Fig. 2C). Importantly, the effect of HMGB2 knockdown was similar to that of HMGB1 knockdown, despite the fact that HMGB2 is a much less abundant protein than HMGB1 (Fig. 2A). The results received after transient knockdown of HMGB1 in human cancer cells are in line with our data obtained in Hmgb1-knockout murine embryonic fibroblasts (5). The present study supports the role of chromatin-associated proteins HMGB1/2 in early steps of drug-induced activation of p53 response by demonstrating delay or abrogation of the stress marker (phosphorylated form of p53) in HMGB1/2-depleted cells (Fig. 3A and C). Our results indicate that HMGB1 (and probably HMGB2) is a sensor of DNA damage which induces p53-mediated DNA damage response. In the cells with depleted HMGB1, manifestation of apoptosis markers (e.g., caspase-mediated PARP proteolysis) is also delayed (Fig. 4). Active scanning for flexible points within DNA as a mechanism of DNA damage detection provides an attractive explanation of how HMGB1 contributes to several seemingly unrelated DNA repair pathways, including mismatch repair, base excision repair, and nucleotide excision repair (21, 22, 27). Of note, DNA substrates of mismatch repair and base excision repair revealed increased flexibility (28–30). Although stimulation of DNA repair by HMGB1 is shown reasonably well, the consequences of HMGB1 depletion for the cells are less clear: no change, decreased, and increased sensitivity to the a panel of DNA-damaging agents was reported in HMGB1 knockout murine embryonic fibroblasts (4, 5, 21, 22, 31). Most interestingly, HMGB1 physically and functionally interacts with p53, indicating a link with p53-dependent signaling networks (32, 33). The intracellular level of HMGB1 is controlled by developmental and tissue-specific factors, and variations in HMGB1 level may explain different sensitivities to chemotherapy in certain cell populations (34). In line with this notion, analysis of gene expression in ovarian tumors indicated a potential association between HMGB1 expression level and resistance to chemotherapy (35).

Depletion of nuclear matrix–associated protein PDIA3 significantly changed chemosensitivity to cytarabine treatment in A549 cell line. Western blot analysis of nuclear extracts from A549 and UO31 cells and immunofluorescent microscopy revealed that knockdown of PDIA3 abrogated the phosphorylation of H2AX (Figs. 3 and 5). Importantly, phosphorylation of the genotoxic marker H2AX occurred independently of p53 phosphorylation: in cells with knocked down PDIA3, phosphorylation of H2AX was significantly

inhibited at 24, 48, and 72 hours, whereas phosphorylation of Ser^{15}-p53 was not affected; this was already observed after 24 hours (Fig. 3). Phosphorylation of p53 and phosphorylation of H2AX are not mutually dependent because phosphorylation of p53 at Ser^{18} (corresponding to Ser^{15} in human p53) and p53 stabilization were normal in *H2AX*$^{-/-}$ murine embryonic fibroblasts and thymocytes after DNA damage, and phosphorylation of H2AX was normal in the human fibroblast cells with compromised p53 (36, 37). Taken together with our observation that abrogation of PDIA3 by RNA interference inhibits phosphorylation of Ser^{139} in H2AX but not Ser^{15} in p53, these facts indicate that phosphorylation of p53 and H2AX occur via independent mechanisms. Although PDIA3 is a member of the protein disulfide isomerase family of proteins mainly present in the endoplasmic reticulum, this protein was found to be associated with the internal nuclear matrix, and its DNA-binding properties have been shown by DNA-protein cross-linking, chromatin immunoprecipitation, and cloning of PDIA3-bound DNA (8, 38). Moreover, PDIA3 was shown to cooperate with Ref-1, a protein involved in DNA repair which is a potent activator of p53 (9, 39). The abrogated phosphorylation of H2AX in PDIA3-depleted cells allows us to assume that PDIA3 participates either in double-strand break formation or H2AX phosphorylation, the hypotheses being investigated in our lab. Accumulation of γ-H2AX is important in establishing a full DNA damage response (40); therefore, PDIA3 could be an important molecular target for enhancing the efficacy of conventional antimetabolite therapy. Additional experiments are needed to assess the exact roles of PDIA3 and HSPA8 in the response to genotoxic stress.

In conclusion, our results, for the first time, show that chromatin-associated HMGB1, HMGB2, and matrix-associated protein PDIA3 in cancer cells are important determinants of cellular response to antimetabolite drugs. Depletion of these proteins in human carcinoma cell lines resulted in the alteration of cellular sensitivity to antimetabolite drugs, and changed manifestation of the cellular stress markers. In this process, proteins have different functions: HMGB1 and HMGB2 facilitate p53 phosphorylation after exposure to genotoxic stress; and PDIA3 has been found to be essential for H2AX phosphorylation. Hence, the phosphorylation of p53 and H2AX occurs in two distinct branches of the DNA damage response. We hypothesize that HMGB1/2 proteins act as a sensor of DNA modification, and their interaction with chemically altered DNA changes the chromatin structure, thus inducing DNA damage response. Elucidation of molecular components of the cell responsive to chemotherapeutic agents will rationalize the strategy for anticancer chemotherapy, and will define molecular markers discriminating between therapeutic failure and success.

Disclosure of Potential Conflicts of Interest

No potential conflicts of interest were disclosed.

Acknowledgments

We are grateful to Nguyen Ngoc for excellent technical assistance. We thank Temple University students Olubunmi Fiki, Robert Tetteh, Hiren Patel, Boris Gankin, Justin Kolb, and Rostislav Meyerzon for their contribution to this project.

References

1. Banerji U, Judson I, Workman P. Molecular Targets. In: Figg WD, McLeod HL, editors. Handbook of anticancer pharmacokinetics and pharmacodynamics. Totowa (NJ): Humana Press; 2004. p. 1–27.

2. Shi Z, Azuma A, Sampath D, Li YX, Huang P, Plunkett W. S-Phase arrest by nucleoside analogues and abrogation of survival without cell cycle progression by 7-hydroxystaurosporine. Cancer Res 2001;61: 1065–72.

3. Bianchi ME, Agresti A. HMG proteins: dynamic players in gene regulation and differentiation. Curr Opin Genet Dev 2005;15:496–506.

4. Krynetski EY, Krynetskaia NF, Bianchi ME, Evans WE. A nuclear protein complex containing high mobility group proteins B1 and B2, heat shock cognate protein 70, ERp60, and glyceraldehyde-3-phosphate dehydrogenase is involved in the cytotoxic response to DNA modified by incorporation of anticancer nucleoside analogues. Cancer Res 2003;63: 100–6.

5. Krynetskaia N, Xie H, Vucetic S, Obradovic Z, Krynetskiy E. High mobility group protein B1 is an activator of apoptotic response to antimetabolite drugs. Mol Pharmacol 2008;73:260–9.

6. Ronfani L, Ferraguti M, Croci L, et al. Reduced fertility and spermatogenesis defects in mice lacking chromosomal protein Hmgb2. Development 2001;128:1265–73.

7. Sirover MA. New nuclear functions of the glycolytic protein, glyceraldehyde-3-phosphate dehydrogenase, in mammalian cells. J Cell Biochem 2005;95:45–52.

8. Chichiarelli S, Ferraro A, Altieri F, et al. The stress protein ERp57/GRP58 binds specific DNA sequences in HeLa cells. J Cell Physiol 2007; 210:343–51.

9. Grillo C, D'Ambrosio C, Scaloni A, et al. Cooperative activity of Ref-1/APE and ERp57 in reductive activation of transcription factors. Free Radic Biol Med 2006;1:1113–23.

10. Tsukahara F, Maru Y. Identification of novel nuclear export and nuclear localization-related signals in human heat shock cognate protein 70. J Biol Chem 2004;279:8867–72.

11. Kodiha M, Chu A, Lazrak O, Stochaj U. Stress inhibits nucleocytoplasmic shuttling of heat shock protein hsc70. Am J Physiol Cell Physiol 2005; 289:C1034–41.

12. Sampath D, Rao VA, Plunkett W. Mechanisms of apoptosis induction by nucleoside analogs. Oncogene 2003;22:9063–74.

13. Ashwell S, Zabludoff S. DNA damage detection and repair pathways-recent advances with inhibitors of checkpoint kinases in cancer therapy. Clin Cancer Res 2008;14:4032–7.

14. Sahasrabudhe PV, Pon RT, Gmeiner WH. Solution structures of 5-fluorouracil-substituted DNA and RNA decamer duplexes. Biochemistry 1996; 35:13597–608.

15. Somerville L, Krynetski EY, Krynetskaia NF, et al. Structure and dynamics of thioguanine-modified duplex DNA. J Biol Chem 2003;278: 1005–11.

16. The Merck Index. 13th ed. Whitehouse Station (NJ): Merck&Co., Inc.; 2001.

17. Freshney RI. Culture of animal cells. 4th ed. New York: Wiley-Liss; 2000.

18. O'Connor PM, Jackman J, Bae I, et al. Characterization of the p53 tumor suppressor pathway in cell lines of the National Cancer Institute anticancer drug screen and correlations with the growth-inhibitory potency of 123 anticancer agents. Cancer Res 1997;57:4285–300.

19. Blumenthal RD. An overview of chemosensitivity testing. In: Blumenthal RD, editor. Methods in molecular medicine. Totowa (NJ): Humana Press; 2005. p. 3–18.

20. Balajee AS, Geard CR. Replication protein A and γ-H2AX foci assembly is triggered by cellular response to DNA double-strand breaks. Exp Cell Res 2004;300:320–34.

21. Prasad R, Liu Y, Deterding LJ, et al. HMGB1 is a cofactor in mammalian base excision repair. Mol Cell 2007;27:829–41.

22. Lange SS, Mitchell DL, Vasquez KM. High mobility group protein B1 enhances DNA repair and chromatin modification after DNA damage. Proc Natl Acad Sci U S A 2008;105:10320–5.

23. Anderson CN, Tolkovsky AM. A role for MAPK/ERK in sympathetic neuron survival: protection against a p53-dependent, JNK-independent induction of apoptosis by cytosine arabinoside. J Neurosci 1999;19:664–73.

24. Lipp HP, Bokemeyer C. Clinical pharmacokinetics of cytostatic drugs: efficacy and toxicity. In: Lipp HP, editor. Anticancer drug toxicity. New York Basel: Marcel Dekker, Inc.; 1999. p. 11–201.

25. Carujo S, Estanyol JM, Ejarque A, Agell N, Bachs O, Pujol MJ. Glyceraldehyde 3-phosphate dehydrogenase is a SET-binding protein and regulates cyclin B-cdk1 activity. Oncogene 2006;25:4033–42.

26. Zheng L, Roeder RG, Luo Y. S phase activation of the histone H2B promoter by OCA-S, a coactivator complex that contains GAPDH as a key component. Cell 2003;114:255–66.

27. Yuan F, Gu L, Guo S, Wang C, Li GM. Evidence for involvement of HMGB1 protein in human DNA mismatch repair. J Biol Chem 2004;279: 20935–40.

28. Obmolova G, Ban C, Hsieh P, Yang W. Crystal structures of mismatch repair protein MutS and its complex with a substrate DNA. Nature 2000; 407:703–10.

29. Lamers MH, Perrakis A, Enzlin JH, Winterwerp HH, de WN, Sixma TK. The crystal structure of DNA mismatch repair protein MutS binding to a G x T mismatch. Nature 2000;407:711–7.

30. Marathias VM, Jerkovic B, Bolton PH. Damage increases the flexibility of duplex DNA. Nucleic Acids Res 1999;27:1854–8.

31. Wei M, Burenkova O, Lippard SJ. Cisplatin sensitivity in Hmbg1−/− and Hmbg1 +/+ mouse cells. J Biol Chem 2003;278:1769–73.

32. Achanta G, Pelicano H, Feng L, Plunkett W, Huang P. Interaction of p53 and DNA-PK in response to nucleoside analogues: potential role as a sensor complex for DNA damage. Cancer Res 2001;61:8723–9.

33. McKinney K, Prives C. Efficient specific DNA binding by p53 requires both its central and C-terminal domains as revealed by studies with high-mobility group 1 protein. Mol Cell Biol 2002;22:6797–808.

34. Guazzi S, Strangio A, Franzi AT, Bianchi ME. HMGB1, an architectural chromatin protein and extracellular signalling factor, has a spatially and temporally restricted expression pattern in mouse brain. Gene Expr Patterns 2003;3:29–33.

35. Bernardini M, Lee CH, Beheshti B, et al. High-resolution mapping of genomic imbalance and identification of gene expression profiles associated with differential chemotherapy response in serous epithelial ovarian cancer. Neoplasia 2005;7:603–13.

36. Kang J, Ferguson D, Song H, et al. Functional interaction of H2AX, NBS1, and p53 in ATM-dependent DNA damage responses and tumor suppression. Mol Cell Biol 2005;25:661–70.

37. Mirzayans R, Severin D, Murray D. Relationship between DNA double-strand break rejoining and cell survival after exposure to ionizing radiation in human fibroblast strains with differing ATM/p53 status: implications for evaluation of clinical radiosensitivity. Int J Radiat Oncol Biol Phys 2006; 66:1498–505.

38. Coppari S, Altieri F, Ferraro A, Chichiarelli S, Eufemi M, Turano C. Nuclear localization and DNA interaction of protein disulfide isomerase ERp57 in mammalian cells. J Cell Biochem 2002;85:325–33.

39. Jayaraman L, Murthy KG, Zhu C, Curran T, Xanthoudakis S, Prives C. Identification of redox/repair protein Ref-1 as a potent activator of p53. Genes Dev 1997;11:558–70.

40. Soutoglou E, Misteli T. Activation of the cellular DNA damage response in the absence of DNA lesions. Science 2008;320:1507–10.